

# Kinetic Constraints in the Phase Transitions of Chemisorbed Carbon Monoxide on Co{10 $\bar{1}$ 0} at High Coverages

J. Gu, Y. Y. Yeo, W. S. Sim,<sup>†</sup> and D. A. King\*

Department of Chemistry, University of Cambridge, Lensfield Road, Cambridge CB2 1EW, U.K.

Received: December 2, 1999; In Final Form: March 7, 2000

The high-coverage structures of CO on Co{10 $\bar{1}$ 0} have been investigated in detail using reflection–absorption infrared spectroscopy (RAIRS) and low-energy electron diffraction (LEED) over the temperature range from 100 to 250 K. This has revealed a curious anomaly. As the coverage is increased above 0.5 monolayer (ML) at temperatures below 250 K, a p(2 $\times$ 1) phase, with atop CO, is incompletely converted to a p(2 $\times$ 1)g phase with a local coverage of 1 ML and CO in bridge sites. At temperatures below 180 K, one-third of the surface is converted into the energetically most stable structure, c(2 $\times$ 6), with CO in two types of bridge sites, local coverage 1.17 ML, and the remaining two-thirds remains in the p(2 $\times$ 1)g phase. On cooling to 100 K, the stable c(2 $\times$ 6) phase is unchanged, still occupying one-third of the surface, and the p(2 $\times$ 1)g phase is transformed to a p(6 $\times$ 1)g phase, driven by vibrational entropy. At these low temperatures, this phase transition occurs between two ordered phases that are both metastable with respect to the high-coverage c(2 $\times$ 6) phase. This is attributed to kinetic constraints within the close-packed adsorbed overlayer associated with frozen-in antiphase domains.

## 1. Introduction

Cobalt has been a well-known Fischer–Tropsch catalyst for over seventy years. However, cobalt single crystal surfaces have not been as widely studied by the various surface science techniques as the neighboring elements in the periodic table (such as Ni and Rh). This may be explained by the challenging task of removing all the bulk impurities, in particular carbon, from the cobalt single crystals. The majority of the limited studies available in the literature for CO adsorption on cobalt is for the {0001} surface,<sup>1–4</sup> and few reports exist for the {10 $\bar{1}$ 0} surface.<sup>5,6</sup>

The {10 $\bar{1}$ 0} plane of hexagonally capped prism (hcp) crystals has a four-layer translational periodicity, the spacing between adjacent layers being alternately short and long. The surface unit cell is analogous to the face-centered cubic (fcc) {110} surface. Full dynamic LEED analyses<sup>7,8</sup> have demonstrated that the equilibrium surface structure is exclusively terminated with the short interlayer spacing outermost and is laterally unreconstructed. Since the hcp {10 $\bar{1}$ 0} surfaces are more open than the fcc {110}, saturation CO coverages greater than 1 monolayer (ML) have been reported. Thus, on Ru{10 $\bar{1}$ 0}, CO molecules can be displaced into the wide, shallow troughs with a saturation coverage of 1.055 ML.<sup>9</sup>

Previously, a RAIRS study of CO adsorption on Co{10 $\bar{1}$ 0} was carried out in combination with LEED and TDS<sup>5</sup> in the temperature range 150–300 K. The following three distinct coverage-dependent phases for CO on Co{10 $\bar{1}$ 0} were identified and characterized. (i) In the fractional coverage range between 0 and 0.5 ML, there is a single desorption peak at  $\sim$ 400 K, associated with a p(2 $\times$ 1) LEED pattern and a C–O stretch in the range of 1972–2020 cm<sup>–1</sup>, attributed to CO in atop sites. A surface structure for this p(2 $\times$ 1) overlayer ( $\theta_{\text{CO}} = 0.5$  ML) was proposed. (ii) Over the range  $0.5 < \theta_{\text{CO}} \leq 1.0$  ML, a second

desorption peak appears at  $\sim$ 340 K, associated with the development of a (2 $\times$ 1)p2mg structure with alternately tilting CO on bridged sites. The bridged CO is distinguished by a C–O stretch at 1900–1967 cm<sup>–1</sup> with a remarkably broad fwhm 29.5–52.5 cm<sup>–1</sup>. In addition, RAIRS data<sup>5,6</sup> show the presence of a small amount of residual atop CO. (iii) Most notably, infrared spectra in the coverage range  $1.0 \leq \theta_{\text{CO}} \leq 1.055$  ML are dominated by a band at 1984 cm<sup>–1</sup> associated with a low-temperature desorption peak at 232 K and a continuously changing LEED pattern that finally develops into a nonprimitive c(2 $\times$ 6) structure. As this happens, the low-coverage atop species is attenuated and there is a 13% reduction in the bridge infrared band intensity compared to the value in the p(2 $\times$ 1)p2mg structure.

Toomes and King proposed a structure for the c(2 $\times$ 6) phase consisting of 3-fold, bridged and atop CO formed by compressing the (2 $\times$ 1)-glide plane overlayer in the [0001] direction, giving a quasi-hexagonal array. However, they were unable to explain the discrepancy between the calculated coverage of 1.17 ML for this c(2 $\times$ 6) phase and the measured 1.055 ML from TPD data.<sup>5</sup>

More recently, complementary LEED and RAIRS studies of a chemisorbed monolayer ( $\theta_{\text{CO}} = 1$  ML) of CO on Co{10 $\bar{1}$ 0} by Gu, Sim, and King (using a greatly improved cooling system), revealed a novel reversible order–order phase transition.<sup>6</sup> When the 1 ML p(2 $\times$ 1)g structure was cooled from 250 to 150 K, there was no change in the RAIR spectrum. However, on further cooling, a new band, associated with 3-fold hollow CO adsorbate, grows in at 1826 cm<sup>–1</sup>. Heating and cooling between 90 and 150 K showed complete reversibility in the RAIR spectra.<sup>6</sup> Below 150 K, a p(6 $\times$ 1)g LEED pattern appears, with missing beams at  $(0, \pm(2n+1)/6)$ . This pattern is sharply developed at 100 K, and further cooling to 90 K gives rise to an additional weaker set of beams at  $(0, \pm(2n+1)/2)$ , indicative of the coexistence of a p(2 $\times$ 1) structure with the p(6 $\times$ 1)g structure.

<sup>†</sup> Present address: Department of Chemistry, National University of Singapore, Kent Ridge, Singapore 119260, Singapore.

The high-temperature phase (150–250 K) consists of tilted 2-fold bridging CO molecules in the  $p(2\times 1)g$  structure, while the low-temperature phase ( $\leq 100$  K) involves the shifting of one-third of the CO molecules into 3-fold hollow sites ( $\sim 1826$   $\text{cm}^{-1}$ ) to produce a new  $p(6\times 1)g$  structure. The temperature-induced site switching was attributed to an order–order displacive phase transition driven by the difference in vibrational entropy between CO on the 2-fold and the 3-fold sites.

Although both the above studies<sup>5,6</sup> provide a detailed description of CO adsorption on  $\text{Co}\{10\bar{1}0\}$ , there are still several unsolved problems. (i) What is the nature of the low-coverage atop adsorption species on the CO-saturated surfaces over the temperature range 180–250 K? (ii) What is the surface structure at high coverages ( $1.0 < \theta_{\text{CO}} \leq 1.055$  ML), related to the appearance of the  $c(2\times 6)$  LEED pattern? (iii) What is the relationship between the  $c(2\times 6)$  phase ( $\theta_{\text{CO}} > 1$  ML) and the  $p(6\times 1)g$  phase ( $\theta_{\text{CO}} \approx 1$  ML) below 150 K?

In the present investigation, with a much improved cooling system, we have applied RAIRS and LEED to examine the different high-coverage CO chemisorption surface structures on  $\text{Co}\{10\bar{1}0\}$  over a broader temperature range (100–250 K) in an attempt to tackle these questions.

## 2. Experimental Details

All the experiments are performed in an ultrahigh vacuum chamber described elsewhere.<sup>5</sup> The essence of the experiments, including some improvements made, are outlined in a recent publication.<sup>6</sup> Essentially, the new liquid nitrogen cooled manipulator assembly, which is a modification of Trenary's original design,<sup>10</sup> allows for more efficient and hence faster cooling to be achieved. The cooling process from 250 to 100 K takes less than 5 min. The heating current is regulated by a Eurotherm controller, which measures the crystal temperature via a chromel–alumel thermocouple attached to the side of the crystal. This chamber is dedicated to UHV studies and has a typical base pressure of  $2 \times 10^{-10}$  mbar. It houses all the standard cleaning and characterization techniques including LEED and TDS.

The system is coupled to a Mattson RS2 FTIR spectrometer via KBr windows. RAIR spectra are recorded typically using 4  $\text{cm}^{-1}$  resolution with 100 scans coadded. All the spectra have been baseline corrected after being ratioed against the background spectra. Each experiment was repeated at least twice and the baseline-corrected spectra were compared to check for the reproducibility of the band positions, intensities, and line shapes. A narrow band MCT detector, operating in the spectral range 4000–800  $\text{cm}^{-1}$ , is used. Only the p-polarized radiation is detected because a polarizer is fitted over the front face of the detector. The spectrometer and the optical path are enclosed and purged with dry nitrogen to remove atmospheric water vapor and  $\text{CO}_2$ , which would otherwise give intense bands.

The  $\text{Co}\{10\bar{1}0\}$  crystal has dimensions of  $15 \times 10 \times 2$  mm and is oriented to within  $0.5^\circ$  of the plane. It is routinely cleaned by repeated cycles of Ar ion sputtering, annealing to 630 K, and oxygen treatment at 400 K—the crystal is never heated above 660 K to avoid the hcp to fcc transition at about 690 K. The resulting clean surface is characterized by sharp LEED patterns and a sharp peak (at 2020  $\text{cm}^{-1}$ ) in the RAIR spectra of CO at 100 K. Any residual carbon or oxygen is readily identified in the RAIR spectra for CO adsorption by the presence of characteristic bands at 2030–2090 and  $\sim 2130$   $\text{cm}^{-1}$ , respectively.<sup>5</sup>

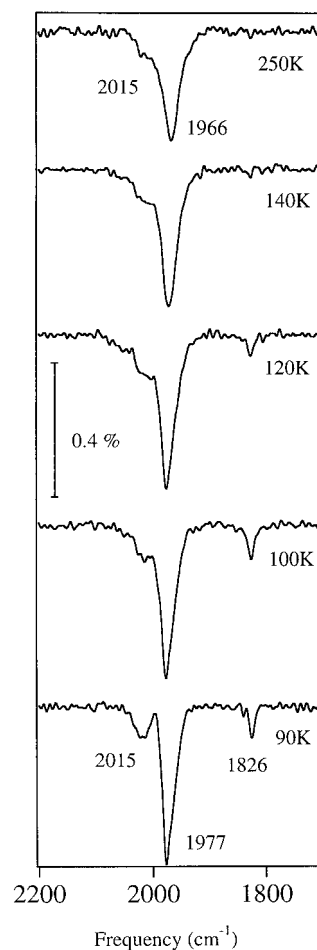


**Figure 1.** RAIR spectra obtained on cooling the  $\text{Co}\{10\bar{1}0\}$  surface previously saturated with CO at 250 K to 90 K.

## 3. Results and Discussion

**3.1.  $\theta_{\text{CO}} \sim 1.0$  ML in the Temperature Range 100–250 K.** As reported by Toomes and King,<sup>5</sup> a small thermal desorption peak observed at 232 K is associated with the appearance of a  $c(2\times 6)$  high-coverage phase on the surface, so we chose 250 K as the CO adsorption temperature to avoid forming the high-coverage phase.

As shown in Figure 1, residual atop CO,  $\nu = 2015$   $\text{cm}^{-1}$ , still exists on the CO-saturated surface at 250 K, and its infrared band intensity is almost not influenced by the order–order phase transition in the temperature range 100–250 K. Moreover, on cooling to 90 K, a further set of weak LEED beams were observed at  $(0, \pm(2n+1)/2)$  suggesting the coexistence of a  $p(2\times 1)$  structure with the  $p(6\times 1)g$  structure. This  $p(2\times 1)$  structure may result from the atop residual species.

The measurement of the infrared spectrum for CO saturation at 250 K indicates that the integrated intensity ratio of the atop to 2-fold bands is around 0.2. However, since the tilting of the 2-fold species will decrease the dynamic dipole normal to the surface, and noting that the magnitude of the dynamic dipole moment may well be different for the two species, we think that it is not suitable to directly relate the intensity ratio to the coverage ratio.

Further, since the atop residue is associated with a  $p(2\times 1)$  structure, a more reasonable method for estimating the relative coverage in the atop species is to use the integrated intensity ratio of the residual atop band to the atop band at  $\theta_{\text{CO}} = 0.5$  ML, when the whole surface has the  $p(2\times 1)$  structure. From this, we deduce that the coverage of the atop species is around

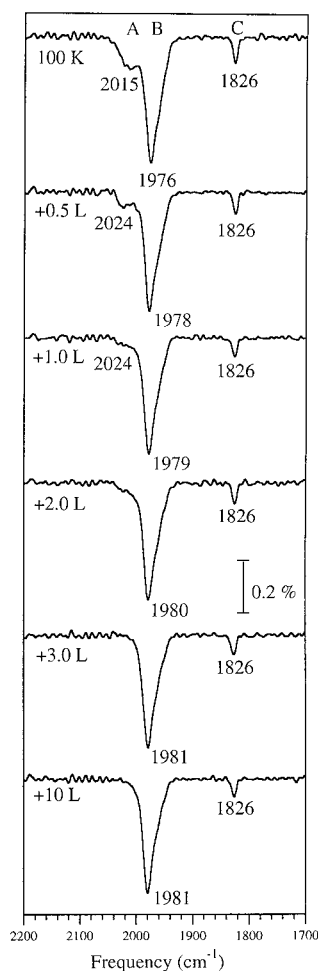


**Figure 2.** RAIR spectral sequence taken after the Co{1010} surface has been CO-saturated at 250 K and cooled to 100 K, with increasing additional exposure to CO.

0.05 ML. Since the local coverage for this structure is 0.5 ML, the atop residue must occupy 10% of the total surface area. We conclude that the coverages of the two CO species at 250 K are atop, 0.05 ML, and 2-fold, 0.9 ML, giving a total of 0.95 ML.

**3.2.  $\theta_{\text{CO}} > 1.0$  ML at 100 K.** It is possible to remove the shoulder at  $2015\text{ cm}^{-1}$  (band A) by dosing more CO onto the 0.95 ML structure at lower temperatures.<sup>5</sup> However, an interesting question is whether the removal of the residual atop species can result in the formation of a uniform 1.0 ML  $p(2\times 1)g$  or  $p(6\times 1)g$  structure.

As shown by Toomes and King,<sup>5</sup> as the crystal is cooled in  $1 \times 10^{-8}$  mbar CO, the atop species, associated with the small shoulder ( $2014\text{ cm}^{-1}$ ), is gradually attenuated from 190 K and almost disappears at 150 K, but meanwhile, a nonprimitive  $c(2\times 6)$  LEED pattern and a third band ( $1980\text{ cm}^{-1}$ ) appear. Since the  $c(2\times 6)$  pattern is associated with the high-coverage phase, this suggests that the removal of the atop species is directly associated with the formation of the high-coverage phase, and thus a uniform 1.0 ML  $p(2\times 1)g$  structure could not be obtained above 150 K.

At 100 K, the  $p(2\times 1)g$  structure formed at 250 K is replaced by the  $p(6\times 1)g$  structure. The  $p(2\times 1)g$  and  $p(6\times 1)g$  LEED patterns are shown in Figure 3a,b, respectively. Since the atop species still exist at 100 K, we exposed the surface to more CO to determine whether a uniform  $p(6\times 1)g$  phase can be formed. Figure 2 shows the RAIRs adsorption sequence obtained for increasing CO exposures on the Co{1010} surface previously

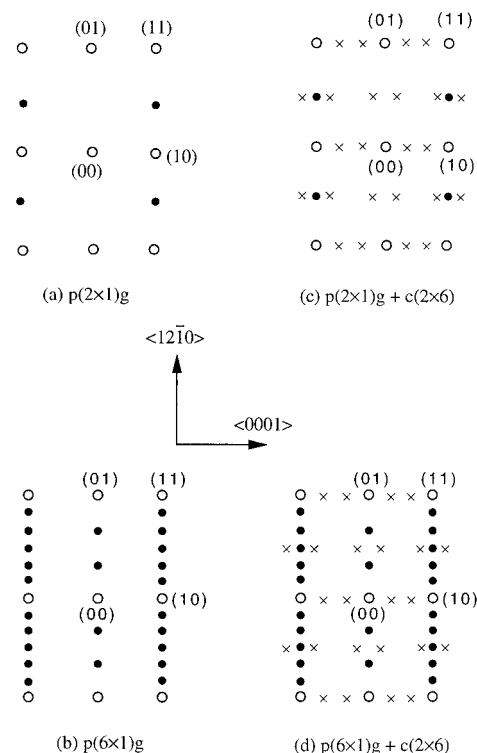


**Figure 3.** Schematic representations of the LEED patterns observed: (a)  $p(2\times 1)g$ ; (b)  $p(6\times 1)g$ ; (c)  $p(2\times 1)g$  and  $c(2\times 6)$ ; (d)  $p(6\times 1)g$  and  $c(2\times 6)$ . Key: (O) integral order beams; (●)  $p(6\times 1)g$  or  $p(2\times 1)g$  phase; (x)  $c(2\times 6)$  phase.

dosed with 30 layers (L) of CO at 250 K and cooled to 100 K. When the additional CO exposure reaches 1.0 L, the intensity of band A diminishes significantly, and at 3.0 L, it disappears completely. On the other hand, with redosing CO up to 3 L, we observe that (i) the sharp and intense peak (band B) from the bridged species shifts only very slightly, from 1976 to  $1981\text{ cm}^{-1}$  (at 3 L, the fwhm of band B is  $\sim 40\text{ cm}^{-1}$  and the band is not symmetric about the peak) and (ii) the intensity of band C for the 3-fold species decreases, while its frequency is unchanged. At saturation, the intensity of band C decreases by about 37%.

LEED patterns were examined carefully under the same conditions as the RAIR spectral sequence of Figure 2. As CO was dosed onto the Co{1010} at 100 K, the background of the  $p(6\times 1)g$  pattern increases. After more than 1.0 L of CO was dosed onto the  $p(6\times 1)g$  structure, additional beams develop at  $(0, \frac{1}{3})$  and  $(\pm\frac{1}{2}, \pm\frac{1}{6})$ . As the exposure of CO increases to 3.0 L, these beams sharpen, and the LEED pattern, as shown in Figure 3d, indicates the coexistence of a nonprimitive  $c(2\times 6)$  structure with a  $p(6\times 1)g$  structure, corresponding to the disappearance of the high-frequency shoulder (band A). In the earlier LEED study,<sup>6</sup> two distinct phases were observed over the temperature range from 100 and 150 K,  $p(2\times 1)g$  at higher temperatures and  $p(6\times 1)g$  at 100 K. No intermediate disordered phase was reported. Here we show that an additional exposure of CO induces the formation of a new nonprimitive  $c(2\times 6)$  phase that coexists with the  $p(6\times 1)g$  structure.

When CO is redosed, the decrease in the intensity of band C shows that the residual atop CO species are not transformed to the  $p(6\times 1)g$  phase. The fraction of the surface occupied by the  $p(6\times 1)g$  phase may even be decreased. Our LEED results indicate that additional LEED spots are observed at low redosing exposures ( $\sim 1$  L), which further confirms the development of a new phase. Therefore, even with careful control of the redosing

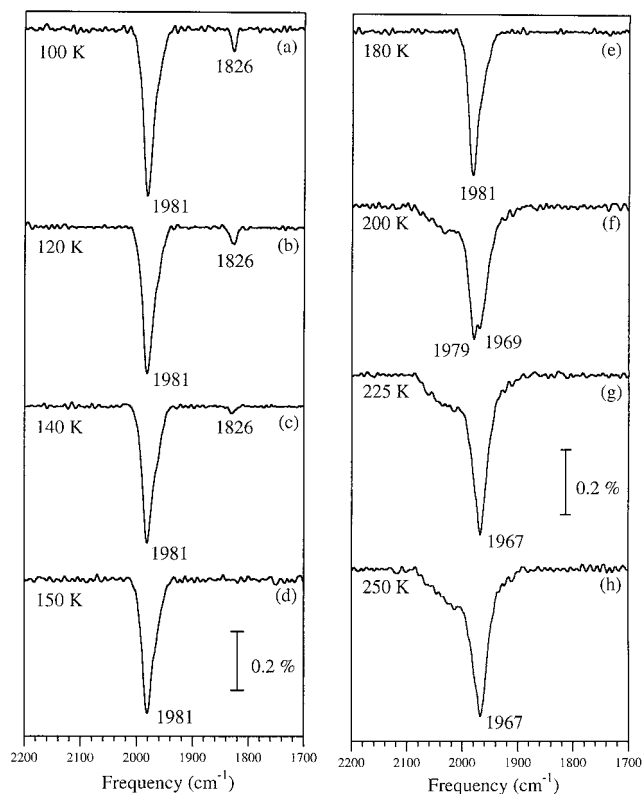


**Figure 4.** RAIR spectra obtained from Co{10 $\bar{1}$ 0} after saturation with CO at 250 K, redosing with a further 10 L exposure of CO at 100 K, and then heating to the temperatures indicated.

exposure to CO, the surface could not be induced to transform fully to the p(6 $\times$ 1)g phase.

**3.3.  $\theta_{\text{CO}} > 1.0$  ML at Increasing Temperatures.** After the surface has been resaturated with CO at 100 K, and the high-frequency shoulder at 2015 cm $^{-1}$  has been removed, increasing the temperature to 250 K produced the following three different transition stages.

(1) 100–180 K. Figure 4a–e shows the RAIRS spectra that were recorded in the temperature range 100–180 K. On heating to 145 K, the intensity of the small peak at  $\sim$ 1826 cm $^{-1}$ , associated with the low-temperature p(6 $\times$ 1)g phase,<sup>6</sup> is gradually attenuated due to the p(2 $\times$ 1)g phase. At 150 K the only feature left in the RAIR spectrum is band B and the frequency of band B remains very constant, at 1981 cm $^{-1}$ . There does appear to be some asymmetry in this peak.

Once again, LEED patterns were observed under identical conditions to correlate with the RAIR spectra. Figure 3d is a schematic representation of the pattern observed at 100 K. With increasing temperature, the p(6 $\times$ 1)g structure becomes more and more dim. At 145 K, when the infrared band corresponding to the 3-fold species has disappeared, the spots at  $((n + 1)/6, \pm 1/3)$  also vanished, and the p(6 $\times$ 1)g is replaced by a p(2 $\times$ 1)g structure, as reported in our previous study.<sup>6</sup> The LEED pattern is shown in Figure 3c. Surprisingly, once formed by saturation exposure at low temperatures ( $\sim$ 100 K), the c(2 $\times$ 6) structure persists up to 220 K.

Most notably, heating and cooling between 100 and 180 K shows complete reversibility in the behavior of both the RAIR spectra and LEED patterns. This suggests that there is no CO desorption between 100 and 180 K, so the coverage of chemisorbed CO is constant. Since the lowest thermal desorption peak is around 232 K, we conclude that there is no difference in the CO coverage between saturating the surface at 140 K as in Toomes and King's work, and at 100 K in our current work.

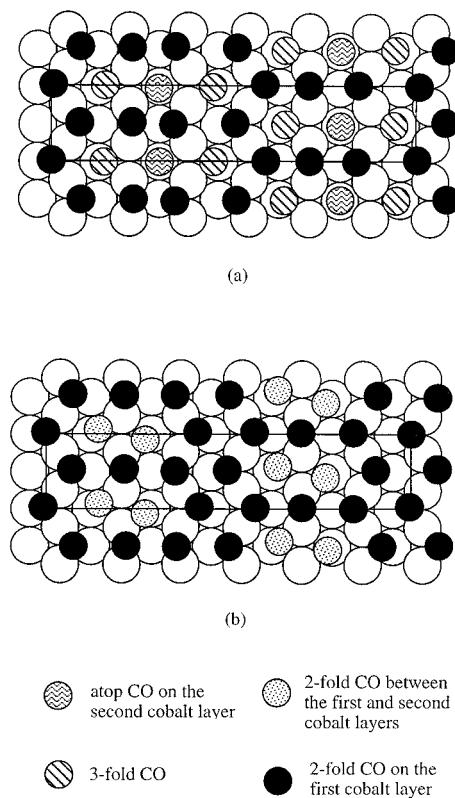


**Figure 5.** Structural models for the incommensurate c(2 $\times$ 6) phase: (a) proposed by Toomes and King;<sup>5</sup> (b) proposed in this work, with the CO molecules adsorbed on two different types of bridge sites—between two Co atoms on the top layer and between a Co atom on the top layer and a Co atom on the second layer.

This should enable us to deduce the saturation coverage at 100 K. Since the new cooling system results in a strong desorption signal from the supports as the temperature starts to increase, we could not get accurate TPD spectra below 250 K to measure the amount desorbed. Toomes and King deduced from their TPD data, however, that the coverage on the CO-saturated surface at 150 K was around 1.055 ML.<sup>5</sup>

(2) 180–225 K. As CO begins to desorb, band B splits into two peaks attributed to bridged species, at 1979 and 1969 cm $^{-1}$ , at 200 K, accompanied by the development of a shoulder at the high-frequency tail. This shoulder is formed as soon as the CO starts to desorb; we were unable to achieve a uniform p(2 $\times$ 1)g phase. The c(2 $\times$ 6) LEED pattern gradually disappears, leaving only the p(2 $\times$ 1)g pattern.

(3) 225–250 K. As the temperature is raised to 225 K, the two bridge bands merge into one band centered at 1967 cm $^{-1}$ , with the shoulder at  $\sim$ 2000–2100 cm $^{-1}$  now more prominent. This broad feature is fully developed at 250 K. Meanwhile, above 225 K, only the p(2 $\times$ 1)g structure is observed. At 250 K, both the RAIR spectra and LEED patterns return to the starting point, where the clean surface was saturated with CO prior to low-temperature redosing. Moreover, the reversible order–order phase transition between 250 and 100 K is now readily repeatable.<sup>6</sup>

We also note that above 145 K our observations are very similar to the previous work done by Toomes and King despite different CO dosing methods.

Toomes and King<sup>6</sup> report that an incommensurate c(2 $\times$ 6) structure is created by compressing the (2 $\times$ 1)-glide plane overlayer in the [0001] direction to give a quasi-hexagonal array in which close-packed CO exhibits a hard-sphere radius of  $\sim$ 1.5 Å. This structure, shown in Figure 5a, consists of a 2-fold bridge



**TABLE 1: Coexistence of Structural CO Phases on Co{10 $\bar{1}$ 0}**

temperature range (K)	$\leq 100$	145–180	220–250
CO coverage (ML)	1.05	1.05	0.95
coexisting CO phases & percentages	$c(2 \times 6) \sim 32\%$ $p(6 \times 1)g \sim 68\%$	$c(2 \times 6) \sim 32\%$ $p(2 \times 1)g \sim 68\%$	$p(2 \times 1) \sim 10\%$ $p(2 \times 1)g \sim 90\%$
type of CO adsorption sites	$c(2 \times 6) \Rightarrow$ [2-fold bridge + 2-fold short bridge]	$c(2 \times 6) \Rightarrow$ [2-fold bridge + 2-fold short bridge]	$p(2 \times 1) \Rightarrow$ [atop]
for different structures	$p(6 \times 1)g \Rightarrow$ [2-fold bridge + 3-fold hollow]	$p(2 \times 1)g \Rightarrow$ [2-fold bridge]	$p(2 \times 1)g \Rightarrow$ [2-fold bridge]

CO on the first cobalt layer, a 2-fold bridge CO between the first and second cobalt layers, and a 3-fold hollow CO and atop CO on the second cobalt layer. However, more information is now extracted from the current data, as shown below.

First, both RAIR spectra and LEED patterns show that above 150 K, with the disappearance of the  $p(6 \times 1)$  pattern, band C (1826  $\text{cm}^{-1}$ ) also vanishes, while the  $c(2 \times 6)$  pattern still exists up to 220 K. This means that the 3-fold hollow species is only associated with the  $p(6 \times 1)$  phase and does not exist in the  $c(2 \times 6)$  structure.

Second, the dominant peak at 1981  $\text{cm}^{-1}$  was observed to split into two distinct peaks at 1979 and 1969  $\text{cm}^{-1}$  when heated from 175 to 200 K. The possibility of this splitting being caused by the  $p(2 \times 1)g$  structure is eliminated because it was not observed when the crystal was saturated at 250 K, cooled to 100 K, and then heated above 220 K.<sup>6</sup> At 175 K, it is evident from the RAIR spectrum that both the  $c(2 \times 6)$  and the  $p(2 \times 1)g$  phase must consist solely of CO molecules populating 2-fold bridge sites. The band splitting at 200 K is therefore attributed to the  $c(2 \times 6)$  phase, which must contain two different kinds of environment for the 2-fold bridge species—probably a short bridge site between the first layer cobalt atoms and a second bridge site between one cobalt atom in the first and the other in the second layer. Because of the close proximity of the two RAIRS peaks, we expect strong coupling and intensity transfer from the 1969 to 1979  $\text{cm}^{-1}$  peak. For this reason it is difficult to relate the peak intensity to the population of each type of CO.

Third, the absence of the high-frequency shoulder below 180 K proves that atop sites are not forming domain walls and that there are no atop species in the  $c(2 \times 6)$  structure.

These results require some modification of the structure proposed by Toomes and King: a new structure for the nonprimitive, incommensurate  $c(2 \times 6)$  phase is shown in Figure 5b, with exclusive population of 2-fold bridge sites. The local coverage for this structure is  $\theta_{\text{CO}} = 1.17$  ML. The average coverage, however, is 1.055 ML.<sup>5</sup> This apparent discrepancy is now resolved, since the  $c(2 \times 6)$  structure does not cover the whole surface; it coexists with the  $p(6 \times 1)g$  phase below 100 K and the  $p(2 \times 1)g$  phase between 150 and 180 K. Since the local coverages for both the  $p(6 \times 1)g$  and  $p(2 \times 1)g$  phases are 1.0 ML, while the local coverage of the  $c(2 \times 6)$  phase is 1.17 ML, the mean coverage  $\theta_{\text{CO}} = 1.055$  ML implies that the surface consists of  $\sim 32\%$  of the  $c(2 \times 6)$  structure and  $\sim 68\%$  of the  $p(6 \times 1)g$  or  $p(2 \times 1)g$  structures. Interestingly, this calculation based on the TPD spectra<sup>5</sup> is further substantiated from the analysis of the infrared spectra in Figure 2. It is found that the decrease in the integrated intensity of band C (1826  $\text{cm}^{-1}$ ) after redosing with CO to saturation is  $\sim 30 \pm 5\%$ . Band C is only associated with the  $p(6 \times 1)g$  phase, and before redosing CO at 100 K, the percentage of the  $p(6 \times 1)g$  phase is around 90%. Therefore, since the integrated intensity of band C should be linearly related to the fraction of the  $p(6 \times 1)g$  phase on the surface, the ratio directly suggests that at saturation the percentage of the  $p(6 \times 1)g$  phase is  $\sim 63 \pm 5\%$ , and thus the

percentage of the  $c(2 \times 6)$  phase is  $\sim 37\%$ . The two estimates are in very satisfactory agreement.

The coexistence of different phases at various temperature regimes is summarized in Table 1. The temperature regime between 100 and 145 K corresponds to the reversible phase transition between the  $p(6 \times 1)g$  and the  $p(2 \times 1)g$  structures.<sup>6</sup> Increasing the temperature from 180 to 220 K is accompanied by partial desorption of CO and the disappearance of the  $c(2 \times 6)$  phase.

**3.4. General Discussion.** In the above we have produced detailed information concerning the coexistence of different phases of adsorbed CO over different temperature regimes. The formation of the  $c(2 \times 6)$  phase only below 200 K shows that it is more stable than the  $p(2 \times 1)g$  phase, and also its counterpart, the  $p(6 \times 1)g$  phase. However, a surprising finding is that although the  $c(2 \times 6)$  phase starts forming on cooling at 200 K with additional CO dosing, the growth of this phase then almost stops at 180 K where it occupies only  $\sim 32\%$  of the surface area, and the remainder is left in the  $p(2 \times 1)g$  phase. Moreover, even on cooling to 90 K, the ratio is unaltered. Therefore, a general question is: why is the  $p(2 \times 1)g \rightarrow c(2 \times 6)$  transition blocked at the point where only  $\sim 32\%$  of the surface is transformed? Thermodynamically, on exposure to more CO, this transition should continue until the whole surface is transformed to a uniform  $c(2 \times 6)$  structure.

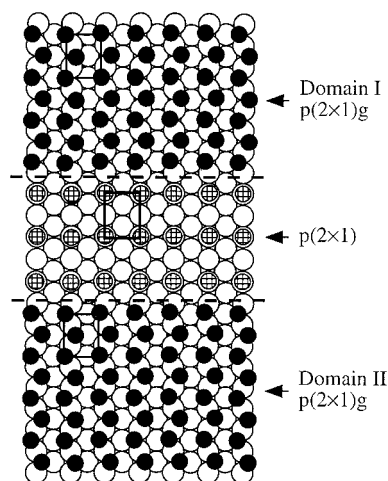
It is likely that this phase transition is kinetically constrained. When the two phases coexist, the surface is composed of multiple domains exhibiting either of the two phases: the boundaries will include antiphase boundaries. We therefore propose the following models for the CO-saturated surface structures at different temperature regimes.

(1) At 220–250 K, where  $\theta_{\text{CO}} = 0.95$  ML,  $p(2 \times 1)g$  domains are separated by  $p(2 \times 1)$  regions, and two  $p(2 \times 1)g$  domains separated by a  $p(2 \times 1)$  region are antiphase to each other. The structure in Figure 6 schematically illustrates this.

(2) At 150–180 K, where  $\theta_{\text{CO}} = 1.055$  ML,  $p(2 \times 1)g$  domains are separated by high-density  $c(2 \times 6)$  regions, and two  $p(2 \times 1)g$  domains separated by a  $c(2 \times 6)$  region are antiphase to each other. The structure in Figure 7a schematically illustrates this.

(3) At 100–150 K, where  $\theta_{\text{CO}} = 1.055$  ML, the  $p(2 \times 1)g \leftrightarrow p(6 \times 1)g$  order–order phase transition occurs,<sup>6</sup> and at 100 K, the transition to  $p(6 \times 1)g$  is complete. However, the  $c(2 \times 6)$  regions are unaltered. This is schematically illustrated in Figure 7b.

The extent of the surface in the most stable  $c(2 \times 6)$  phase is frozen at  $\sim 32\%$ . We note that the transition between  $p(6 \times 1)g$  and  $p(2 \times 1)g$  phases on the remaining  $\sim 68\%$  of the surface is facile: it simply requires the movement of  $1/3$  of the molecules from 3-fold to neighboring bridge sites. This requires a small activation barrier to be surmounted. But the growth of the  $c(2 \times 6)$  phase into either of these phases, across antiphase boundaries, would require a substantial cooperative rearrangement of the adsorbed layer. Since these phase boundaries are frozen in place at temperatures as high as 180 K, we conclude that this process is hindered by an activation barrier in the region



⊕ on-top CO on the first cobalt layer      ● 2-fold CO on the first cobalt layer

Figure 6. Domain wall structure for  $p(2 \times 1)g$  at 250 K.

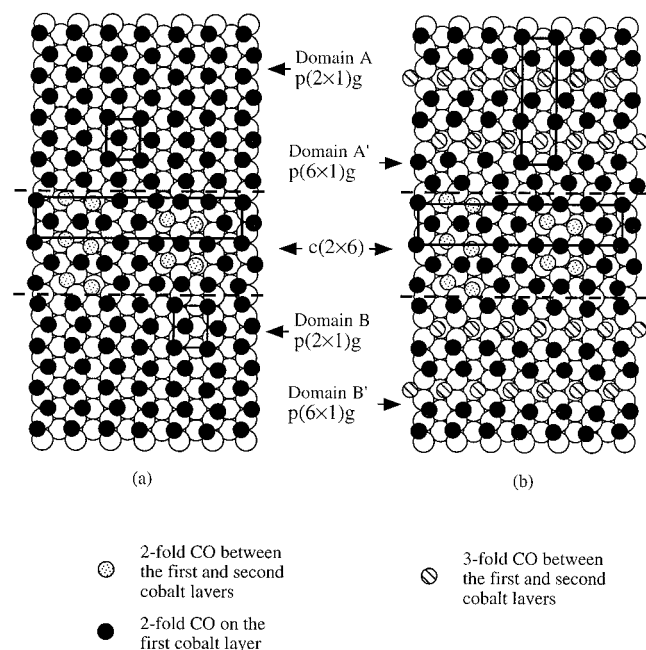


Figure 7. (a) Domain wall structure for  $p(2 \times 1)g$  and  $c(2 \times 6)$ . (b) Domain wall structure for  $p(6 \times 1)g$  and  $c(2 \times 6)$ .

of  $50 \text{ kJ mol}^{-1}$ . At these high coverages, mobility in the adlayer is severely hindered, and the  $p(6 \times 1)g/p(2 \times 1)g$  region of the surface is locked into a metastable state.

Experimentally, the existence of domains is supported by the relatively large fwhm of the 2-fold bridge band (band B). Usually, sharp LEED patterns are associated with narrow C—O stretching bands and a well-ordered overlayer. For example, this is the case for the  $(2 \times 1)p2mg$  structure on  $\text{Ni}\{110\}$  for which the fwhm of the band at  $1998 \text{ cm}^{-1}$  is  $7 \text{ cm}^{-1}$ .<sup>11</sup> Here, although CO saturation on  $\text{Co}\{10\bar{1}0\}$  at 250 K produces a sharp, intense  $p(2 \times 1)g$  LEED pattern with a low background, band B,  $1967\text{--}1981 \text{ cm}^{-1}$ , associated with the  $(2 \times 1)p2mg$  structure, has a minimum fwhm of  $\sim 30 \text{ cm}^{-1}$ . A reasonable explanation is that the presence of many  $p(2 \times 1)g$  domains causes inhomogeneous broadening in the fwhm.

#### 4. Conclusion

High-coverage surface phases for CO on  $\text{Co}\{10\bar{1}0\}$  ( $0.95 \leq \theta_{\text{CO}} \leq 1.055 \text{ ML}$ ) have been identified and characterized by the combination of RAIRS and LEED over the temperature range between 100 and 250 K. At most temperatures, two different ordered phases can coexist on CO-saturated  $\text{Co}\{10\bar{1}0\}$ , attributable to kinetic constraints. An antiphase domain wall model is proposed to explain this constraint at high coverages.

It is found that when a small amount of CO is dosed at 100 K onto  $\text{Co}\{10\bar{1}0\}$  previously saturated at 250 K with  $\theta_{\text{CO}} = 0.95$ , all the residual atop CO species and part of the  $p(6 \times 1)g$  phase are transformed to a new  $c(2 \times 6)$  phase. At saturation the surface coverage reaches  $\theta_{\text{CO}} = 1.055$ , and it consists of  $\sim 32\%$   $c(2 \times 6)$  phase with a local coverage of 1.17 ML, and  $\sim 68\%$   $p(6 \times 1)g$  phase with a local coverage of 1.0 ML. For  $100 \leq T \leq 150 \text{ K}$ , a reversible order—order phase transition is observed in the  $p(6 \times 1)g$  phase. At 150 K the  $p(6 \times 1)g$  phase is completely replaced by a  $p(2 \times 1)g$  phase, while the  $c(2 \times 6)$  phase remains to 220 K. For  $150 \leq T \leq 180 \text{ K}$ , the coverage of  $\theta_{\text{CO}}$  is still 1.055, and the surface consists of  $\sim 32\%$   $c(2 \times 6)$  phase and  $\sim 68\%$   $p(2 \times 1)g$  phase. The infrared spectra from 100 to 180 K are dominated by a peak at  $1981 \text{ cm}^{-1}$ , which is assigned to bridged CO. A small peak at  $1826 \text{ cm}^{-1}$  is also observed and is attributed to the presence of 3-fold CO in the  $p(6 \times 1)g$  phase. With increasing temperature from 180 to 220 K, some CO desorbs and the  $c(2 \times 6)$  structure disappears. The LEED patterns change continuously and are accompanied by an evident splitting of the  $1981 \text{ cm}^{-1}$  peak into two peaks at 1979 and  $1969 \text{ cm}^{-1}$ , clearly indicating that the  $c(2 \times 6)$  phase contains two different bridged species. Surface structures for CO at different temperature ranges are proposed, which include the antiphase domain walls. The incomplete phase transition from the  $p(2 \times 1)g$  (or  $p(6 \times 1)g$ ) to the  $c(2 \times 6)$  phase at temperatures below 180 K is attributed to kinetic constraints within the close-packed overlayer, possibly associated with the development of these frozen-in antiphase domain boundaries.

**Acknowledgment.** We acknowledge the EPSRC for an equipment grant, the Cambridge Overseas Trust, King's College Cambridge, and the Department of Chemistry for a joint scholarship (J.G.) and the Oppenheimer Fund for Research Fellowships (W.S.S and Y.Y.Y.). We are very grateful to Dr. Adrian Wander for helpful discussions concerning the interpretation of LEED patterns.

#### References and Notes

- (1) Bridge, M. E.; Comrie, C. M.; Lambert, R. M. *Surf. Sci.* **1977**, *67*, 393.
- (2) Papp, H. *Surf. Sci.* **1983**, *129*, 205.
- (3) Greuter, F.; Heskett, D.; Plummer, E. W.; Freund, H.-J. *Phys. Rev. B* **1983**, *27*, 7117.
- (4) Lahtinen, J.; Vaari, J.; Talo, A.; Vehanen, A.; Hautojärvi, P. *Vacuum* **1990**, *41*, 112.
- (5) Toomes, R. L.; King, D. A. *Surf. Sci.* **1996**, *349*, 1.
- (6) Gu, J.; Sim, W. S.; King, D. A. *J. Chem. Phys.* **1997**, *107*, 5613.
- (7) Lindroos, M.; Barnes, C. J.; Hu, P.; King, D. A. *Chem. Phys. Lett.* **1990**, *173*, 92.
- (8) Over, H.; Kleinle, G.; Ertl, G.; Moritz, W.; Wohlgemuth, H.; Christmann, K.; Schwarz, E. *Surf. Sci.* **1991**, *254*, L469.
- (9) Lauth, G.; Solomun, T.; Hirschwald, W.; Christmann, K. *Surf. Sci.* **1989**, *210*, 201.
- (10) Brubaker, M. E.; Trenary, M. *J. Chem. Phys.* **1986**, *85*, 6100.
- (11) Haq, S.; Love, J. G.; King, D. A. *Surf. Sci.* **1992**, *275*, 170.